Effect of Pore Pressure on Damage Accumulation in Salt

T. W. Pfeifle[a] and L. D. Hurtado[b]

[a]RESPEC
P. O. Box 725, Rapid City, South Dakota, U.S.A.

[b]Sandia National Laboratories,
M. S. 1010, P. O. Box 5800, Albuquerque, New Mexico, U.S.A.

Laboratory data acquired from two multistage triaxial compression creep experiments are presented for bedded salt. The experiments were conducted to study the effect of pore pressure changes on the accumulation of damage (dilatant volumetric strain). The first experiment comprised five constant total stress tests in which the internal pore pressure was incremented during successive stages, while the externally applied axial and radial stresses were maintained constant. The second experiment comprised two constant effective stress tests in which the pore pressure and the externally applied axial and radial stresses were increased in equal increments in successive stages. Volumetric strain rates were determined both before and after the pore pressure changes were made in all tests. The data suggest pore pressure changes made during the constant total stress tests have a greater effect on salt dilation than do changes made during the constant effective stress tests.

1. BACKGROUND

The excavation of an underground opening in salt alters the state of stress in the adjacent host rock from a hydrostatic (or nearly hydrostatic) condition to one of shear because of the stress concentrating effect of the opening. When the mean stress in the salt is low relative to the induced shear or deviatoric stress, microfractures initiate in the salt and grow with time, particularly if no back pressure is applied to the excavated surfaces of the opening. The microfractured zone around the opening is often referred to as the damaged or disturbed rock zone (DRZ) and is characterized by the development of new porosity which results in an increase in both bulk volume (i.e., dilation) and permeability [1, 2].

Fluid (e.g., brine, oil, or gas) may fill the newly created porosity of the DRZ and can become pressurized over time through natural and/or operational processes. Traditionally, the effect of the pore fluid pressure on the mechanical and hydrologic properties of salt has been ignored because rock salt was assumed to be impermeable; however, this assumption may not be valid for the salt within the DRZ. Fokker et al. [3] recently examined the effect of pore pressure on the confined strength and permeability of salt and showed that strength decreases and permeability increases with increases in pore pressure. Furthermore, the confined compressive strength of salt was shown to be approximately equivalent to its unconfined strength when the pore pressure and confining pressure were equal. Based on these results, Fokker et al. [3] suggested the use of the well known Terzaghi effective stress concept for characterizing salt strength.

The aim of this paper is to extend and complement the work of Fokker et al. [3] by investigating the effect of pore pressure on damage accumulation in salt under conditions of both constant total stress and constant effective stress creep loading.

2. TECHNICAL APPROACH

The effect of pore pressure on damage accumulation in salt was studied by conducting two multistage creep experiments under stress and temperature conditions known to induce microfracturing. The experiments made use of standard triaxial com-

pression equipment and cylindrical test specimens. Both experiments used nitrogen gas for the pore fluid and a common temperature of 25°C.

The first experiment comprised five two-stage constant total stress (CTS) tests in which the stresses applied to the external surfaces of the specimen were held constant while the pore pressure was incremented from one stage to the next. In both stages of these tests, the axial and radial stresses were 21 MPa and 1 MPa, respectively, so the applied stress difference (axial stress minus radial stress) was 20 MPa. The pore pressure was 0 MPa during the first stage of the test, but was incremented to either 0.4 MPa or 0.8 MPa during the second stage so the effective stress (i.e., total stress minus pore pressure) decreased from one stage to the next. For example, the effective radial stress decreased from 1 MPa to either 0.6 MPa or 0.2 MPa.

The second experiment comprised two four-stage constant effective stress (CES) tests. The stress and temperature conditions during the first stage of each of these tests were identical to those used in the first stage of the CTS tests. However, in the subsequent three stages of the CES tests, the axial stress, radial stress, and pore pressure were all incremented by 1 MPa, 3 MPa, and 7 MPa above their respective Stage 1 values. Thus, the effective stress was maintained constant from one stage to the next.

A single-stage creep test was also performed at a stress difference of 20 MPa, a confining pressure of 1 MPa, and a temperature of 20°C. This test was a control test serving to provide the baseline deformation characteristics of the salt under zero pore pressure conditions.

Axial and radial deformations were measured during both experiments and then converted to true (logarithmic) strains. Volumetric strain, calculated from the axial and radial true strains, was the measure used to characterize damage and its accumulation with time. Volumetric strain rates were determined both before and after the pore pressure changes were made to assess the effect of the change on damage accumulation.

3. EXPERIMENTAL METHOD

3.1 Test specimens

The test specimens used in the study were prepared from bedded salt samples recovered from a depth of approximately 660 meters from the Waste Isolation Pilot Plant (WIPP)* located near Carlsbad, New Mexico. The preparation process required: (1) subcoring of the field samples using a standard rock coring barrel mounted in a vertical milling machine, (2) sawing the ends to approximate length using an ordinary band saw, and (3) finishing the ends flat and parallel in a lathe using carbide tools. The process produced cylindrical specimens nominally 200 millimeters long by 100 millimeters in diameter.

Each specimen was placed between two metal endcaps. The exposed surfaces of the specimen were covered by a flexible Viton tube or jacket that was secured to the endcaps with lockwire. During testing, the flexible jacket provided a barrier between the specimen and the silicone oil used as the confining pressure medium. The metal endcaps were equipped with 4.8-millimeter-diameter vent holes drilled coincident with the central axis of the endcaps to allow pore fluid to enter the ends of the specimen during testing. Thin porous felt metal disks were placed in the interfaces between the specimen and the endcaps to distribute gas uniformly across both ends of the specimen.

Each specimen was subjected to a hydrostatic consolidation stress of 30 MPa before the creep testing was conducted. The consolidation phase had a duration of at least 3 days and was designed to close and potentially heal any damage that may have been induced in the salt during the specimen preparation activities. Specimen dimensions were accurately measured following the consolidation phase and also after each stage of the creep tests.

3.2 Test equipment and instrumentation

Both the CTS and CES experiments were conducted using six standard triaxial compression testing machines. These machines comprise: (1) a pressure vessel for applying radial stress (or confining pressure), (2) a hydraulic cylinder for applying axial load, and (3) a load frame for reacting the applied axial load. The machines are configured so that two of the three principal stresses are identical and equal in magnitude to the radial stress. The third principal stress is equal to the axial stress applied to the ends of the specimen. Minor modifications were made to the pressure vessels of all six machines to allow for

* The U. S. Department of Energy operates the WIPP as the first licensed repository for the disposal of transuranic radioactive wastes produced from defense activities and their funding of this study is acknowledged.

internal pore pressure. The modifications included the installation of high-pressure stainless steel tubing between a pressurized nitrogen gas reservoir and the ports in the pressure vessel connected to the specimen endcaps. The gas reservoir was equipped with a valve for regulating the gas pressure supplied to the specimen. A pressure transducer for monitoring the gas pressure was placed in the high-pressure line near the ports of the pressure vessel.

During testing, electronic transducers were used to measure axial load, radial stress, pore pressure, temperature, and axial and radial displacements. These transducers were calibrated using standards certified by the National Institute for Standards and Technology.

3.3 Test procedure

The first stage of all creep tests was performed according to a common set of procedures. First, the specimen was placed inside the pressure vessel and the annulus between the specimen and vessel walls was filled with silicone oil. Then, the silicone oil was pressurized to 1 MPa (inducing a hydrostatic stress of 1 MPa on the specimen) and heated to a temperature of 25°C. When the pressure and temperature had stabilized, a stress difference ($\Delta\sigma$) of 20 MPa was applied to the specimen by increasing the axial stress (σ_a) to 21 MPa and maintaining the radial stress (σ_r) at the initial hydrostatic value. The axial force applied to the ends of the specimen was continuously adjusted during the stage to account for changes in specimen diameter, thereby ensuring the axial stress remained constant. Axial and radial deformations were measured with time under these constant stress and temperature conditions. When the deformation rates reached steady state (or nearly so), the stage was terminated.

For subsequent stages of the tests, the specimen was placed back in the pressure vessel and heated using the procedure described above for the first stage. Then, the hydrostatic stress and pore pressure were applied simultaneously. In the CTS tests, the hydrostatic stress in the second stage was 1 MPa and the pore pressure (P_p) was nominally 0.4 MPa or 0.8 MPa. In the CES tests, the hydrostatic stresses in the second, third, and fourth stages were 2 MPa, 4 MPa, and 8 MPa, while the corresponding pore pressures were 1 MPa, 3 MPa, and 7 MPa. The pore pressure was applied by adjusting the regulator valve on the gas reservoir using the output of the pore pressure transducer as feedback. When the hydrostatic stress and pore pressure had stabilized, a stress difference of 20 MPa was again applied to the specimen.

The target value for the axial stress in the second stage of the CTS tests was 21 MPa (exactly the same as in the first stage of loading because the radial stress remained constant from stage to stage). However, in the three subsequent stages of the CES tests, the target values for the axial stress were 22 MPa, 24 MPa, and 28 MPa to account for the higher radial stresses (i.e., 2 MPa, 4 MPa, and 8 MPa) specified for these stages. Axial force was adjusted to account for changes in specimen diameter. Axial and radial deformations were again measured with time and the stages were terminated when the deformation rates reached steady state.

4. RESULTS

In analyzing the data from each of the CTS and CES tests, the measured axial and radial true (or logarithmic) strains (ε_a and ε_r) were used to calculate the volumetric strain, ε_v, according to:

$$\varepsilon_v = \varepsilon_a + 2\varepsilon_r \qquad (1)$$

Compressive strains were signed positive so negative values of volumetric strain indicated dilation. The volumetric creep strains were plotted as functions of time for each test to assess, qualitatively, the effect of changes in pore pressure on volumetric strain (or accumulated damage). Figures 1 and 2 plot, respectively, the volumetric strain versus time curves for the two CES tests and the three CTS tests conducted at a nominal pore pressure of 0.8 MPa. The volumetric strain versus time curve for the control test is also shown in these figures for comparison. Arrows drawn in both figures indicate the beginning of subsequent test stages.

The volumetric strains shown in Figure 1 for the first stage of each CES test and the control test exhibit large differences that are attributed to specimen-to-specimen variation. Of most interest, however, is the response of the volumetric strain versus time curve immediately following changes in pore pressure (i.e., when new stages are initiated). As shown, the volumetric strain rate remains virtually constant in both tests after the pore pressure changes are made. This observation is quantified by comparing the ratios of the volumetric strain rate determined after the pore pressure was incremented to the corresponding rate determined at the end of the first

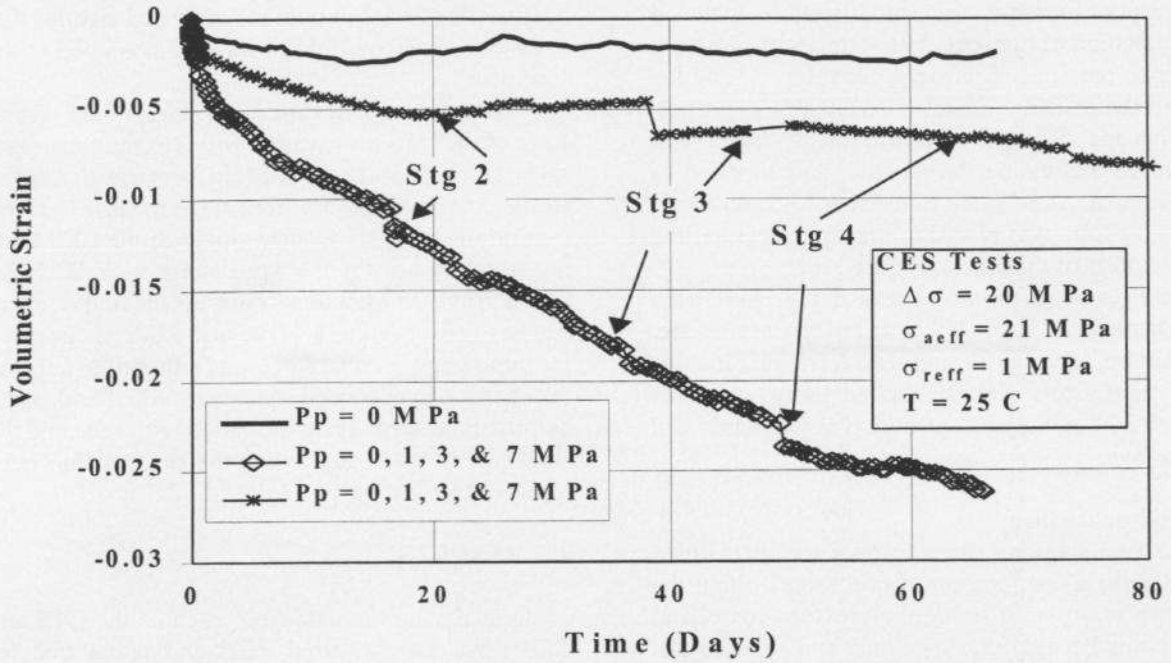

Figure 1. Volumetric strain versus time for constant effective stress creep tests. (Note: Each curve represents a different test specimen.)

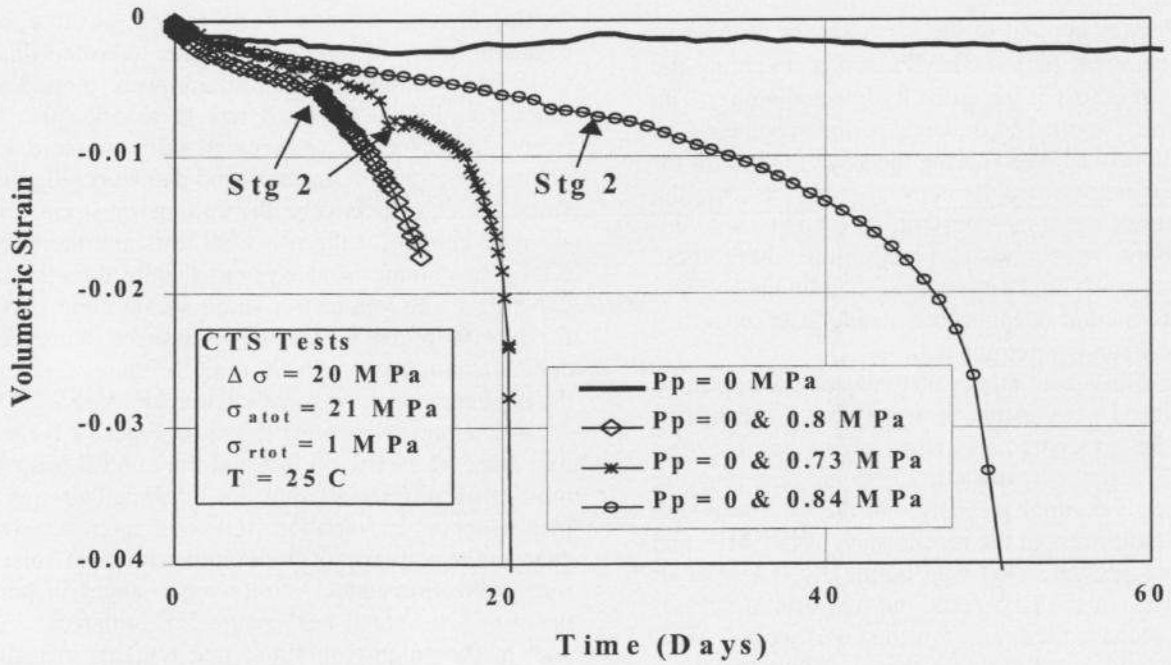

Figure 2. Volumetric strain versus time for constant total stress creep tests conducted at a nominal pore pressure of 0.8 MPa. (Note: Each curve represents a different test specimen.)

Table 1
Summary of volumetric strain rates determined for CES and CTS creep tests on bedded salt

Test	Test Stage	Total Axial Stress (MPa)	Total Radial Stress (MPa)	Pore Pressure (MPa)	Volumetric Strain Rate (1/s)	Volumetric Strain Rate Ratio[a]
CES1	1	21	1	0	–3.70 E-09	—
	2	22	2	1	–3.94 E-09	1.06
	3	24	4	3	–3.70 E-09	1.00
	4	28	8	7	–3.59 E-09	0.97
CES2	1	21	1	0	–1.04 E-09	—
	2	22	2	1	4.60 E-10	-0.44
	3	24	4	3	–8.10 E-10	0.78
	4	28	8	7	–2.31 E-10	0.22
CTS1	1	21	1	0	–2.55 E-09	—
	2	21	1	0.36	–1.27 E-09	0.50
CTS2	1	21	1	0	–7.18 E-10	—
	2	21	1	0.41	–8.22 E-10	1.14
CTS3	1	21	1	0	–3.70 E-09	—
	2	21	1	0.8	–1.75 E-08	4.73
CTS4	1	21	1	0	–6.94 E-09	—
	2	21	1	0.73	–8.68 E-09	1.25[b]
CTS5	1	21	1	0	–3.01 E-09	—
	2	21	1	0.84	–4.63 E-09	1.54[b]

[a] The ratio of the volumetric strain rate determined immediately following a pore pressure change and the volumetric strain rate determined at the end of the first stage of loading.
[b] Specimens used in these tests failed through creep rupture mechanisms.

stage before any pore pressure was induced in the specimen. The strain rates were determined by fitting a straight line to volumetric strain creep data using linear least squares. Table 1 provides a summary of the volumetric strain rates and the strain rate ratios. The strain rates determined after the pore pressure changes were made are shown to be about the same as, or somewhat lower than, the initial strain rates, indicating that pore pressure has little effect on volumetric straining of salt in the CES tests.

Figure 2 presents the volumetric creep strain versus time curves for the three CTS tests conducted at a nominal pore pressure of 0.8 MPa and the control test. Less specimen-to-specimen variability is observed for these data as compared to the CES test data. In addition, the strain rates observed after the pore pressure is introduced into the specimen are higher than at the end of the first stage. The ratios of these strain rates are also shown in Table 1. In one test, the strain rate increases by a factor of nearly five. In the other two tests, the strain rate increase ranges from about 25 to 50 percent. In both of these tests, the volumetric strain rate accelerates and, as shown in Figure 2, the specimens fail by creep rupture.

Table 1 also provides the volumetric strain rates and strain-rate ratios for the two CTS tests conducted at a nominal pore pressure of 0.4 MPa. In contrast to the results obtained for the CTS tests at the higher pore pressure, the volumetric strain rate ratios for these two tests are 0.5 and 1.14, indicating that pore pressure has little or no effect on the volumetric strain rate under CTS conditions.

Hydrologically speaking, natural rock salt is considered to be extremely tight having an intrinsic permeability of less than 1×10^{-21} m^2, so questions arise as to whether the pore pressure applied during these experiments was equally distributed through-

out the matrix of the test specimens. Permeability provides a measure for resolving this concern, but no tests were performed in the study to characterize the permeability of the test specimens as damage accumulated with time. Fortunately, Pfeifle et al. [2] have correlated the permeability of WIPP salt to volumetric strain. Although undamaged WIPP salt is extremely tight, the permeability increases dramatically with small increases in dilatant volumetric strain. For instance at a dilatant volumetric strain of 0.5 percent, the permeability of WIPP salt is approximately 1×10^{-14} m^2. The permeability increases to nearly 1×10^{-12} m^2 for dilatant volumetric strains of 2.5 percent or more. As shown in Figures 1 and 2, the dilatant volumetric strain at the beginning of the second stage of loading ranged from about 0.5 percent to 1 percent, which implies the permeability of the test specimens when the pore pressure is introduced is at least 1×10^{-14} m^2. Theoretically, the gas should be uniformly dispersed throughout the specimen based on these higher permeabilities; however, the damage induced by the imposed stress state may be preferentially oriented so distribution of the gas pressure may still be a concern.

5. SUMMARY AND CONCLUSIONS

Two multistage triaxial compression creep experiments were conducted to study the effect of pore pressure changes on the accumulation of damage (dilatant volumetric strain) in bedded salt. The first experiment comprised five constant total stress tests in which the internal pore pressure was incremented while the externally applied stresses were held constant. The second experiment comprised two constant effective stress tests in which the pore pressure and externally applied stresses were increased in equal increments in successive stages. The effect of the changes in pore pressure on volumetric strain were quantified by estimating the volumetric strain rate at the end of the first stage of loading and comparing this rate to the volumetric strain rates determined immediately after the pore pressure was incremented.

Although only limited testing was performed, a number of observations and conclusions can be drawn from the study including:

1. Increases in pore pressure do not significantly affect volumetric straining in salt provided constant effective stress conditions are maintained.
2. Tests conducted under constant total stress conditions at low effective radial stresses (0.2 MPa or less) suggest that increases in pore pressure increase the volumetric straining of salt which could, ultimately, lead to failure through a creep rupturing mechanism.
3. In contrast, other tests conducted under constant total stress conditions at moderate effective radial stresses (0.6 MPa) suggest that increases in pore pressure have little affect on the volumetric straining of salt.

These conclusions do not imply there is a theoretical effective stress threshold value (of say 0.2 MPa) that controls volumetric straining of salt. Instead, it is likely that the salt response changes significantly as effective radial stress (or effective confining pressure) increases from zero to some small value, and less significantly with further increases in effective stress. The studies of Fokker et al. [3] also showed dramatic changes in salt behavior when the effective stress was very near zero.

Other variables may affect the relationship between pore pressure and damage. These variables were not investigated but may include the physical characteristics of the salt (e.g., initial porosity) and the level of damage induced in the salt before the pore pressure is applied. Further studies are recommended to supplement and expand this limited database and to investigate the effects of other variables.

REFERENCES

1. J. C. Stormont, C. L. Howard, and J. J. K. Daemen. *In Situ Measurements of Rock Salt Permeability Changes Due to Nearby Excavations*, SAND90-3134 (1991).
2. T. W. Pfeifle, N. S. Brodsky, and D. E. Munson. "Experimental Determination of the Relationship Between Permeability and Micro-Fracture Induced Damage in Bedded Salt," *Proceedings, 3rd North American Rock Mechanics Symposium*, Cancún, Mexico (1998), Paper No. 324-1.
3. P. A. Fokker, C. J. Kenter, and H. P. Rogaar. "The Effect of Fluid Pressures on the Mechanical Stability of (Rock) Salt," *Proceedings, 7th Symposium on Salt* (1992).